Harvestable vibrational energy from an avian source: theoretical predictions vs. measured values

Michael W. Shafer[a], Robert MacCurdy[a], Ephrahim Garcia[a], David Winkler[b]

[a]Sibley School of Mechanical and Aerospace Engineering,
Cornell University, Upson Hall, Ithaca, NY, USA;
[b]Department of Ecology and Evolutionary Biology,
Cornell University, Thurston Hall, Ithaca, NY, USA;

ABSTRACT

For many reasons, it would be beneficial to have the capability of powering a wildlife tag over the course of multiple migratory seasons. Such an energy harvesting system would allow for more data collection and eliminate the need to replace depleted batteries. In this work, we investigate energy harvesting on birds and focus on vibrational energy harvesting. We review a method of predicting the amount of power that can be safely harvested from the birds such that the effect on their longterm survivability is not compromised. After showing that the safely harvestable power is significant in comparison to the circuits used in avian tags, we present testing results for the flight accelerations of two species of birds. Using these measured values, we then design harvesters that matched the flight acceleration frequency and are sufficiently low mass to be carried by the birds.

Keywords: bird, tag, energy harvesting, piezoelectric

1. INTRODUCTION

The tags used to monitor wildlife can either be passive or active. Passive tags simply identify an individual, whereas active tags may send out a radio beacon or even collect data. These active tags are typically battery powered, and thus have limited life. This is especially true for birds given their limits on excess payload capacity. We are interested in extending the life of these tags by harvesting energy from the bird and converting it to stored energy on a battery. This stored energy could then be used to collect environmental data, location data, transmit stored data, and possibly take in-situ physiological measurements for the bird. In this work we make predictions for the safely harvestable power from a bird, and use recorded flight accelerations measurements to design an appropriately size a piezoelectric based vibrational energy harvester.

This paper is divided into three major sections. We first review a method[1] for predicting the harvestable power based on the power required for flight. This method converts the bird's maximum allow payload capacity into an energy value that can be safely harvested. We then give an overview of bird flight testing which was conducted in order to obtain the necessary parameters required for development of a piezoelectric based vibrational energy harvester. In these tests, accelerometers were fixed to birds that flew within a bird flight wind tunnel. The results allow for determination of acceleration fundamental frequency and magnitude, two variables needed for energy harvester design.

The last major section uses the results of the bird flight test to aid in the design of an energy harvester beam. The energy harvesters considered here are piezoelectric bimorph resonators. An example of how such an energy harvester could be implemented can be see in figure 1. These energy harvesting systems convert mechanical energy input through base excitation to electrical energy. The motion at the base of the beam, in this case provided by the flight of the bird, excites the fundamental resonance of the beam. At resonances, the beam develops stress in the laminated piezoelectric layers. This stress results in charge accumulation across the

Further author information: (*Send correspondence to M.W.S.)
M.W.S.: E-mail: mws228@cornell.edu, Telephone: 1 607.255.5457
R.M.: E-mail: rbm7@cornell.edu , Telephone: 1 607.254.2102
E.G.: E-mail: eg84@cornell.edu , Telephone: 1 607.255.4366
D.W.: E-mail: dww4@cornell.edu , Telephone: 1 607.254.4216

Active and Passive Smart Structures and Integrated Systems 2012,
edited by Henry A. Sodano, Proc. of SPIE Vol. 8341, 834103 · © 2012 SPIE
CCC code: 0277-786X/12/$18 · doi: 10.1117/12.915370

piezoelectric material that can be used to charge a battery or directly power a system such as these wildlife tracking tags. In this final section of the paper, use the testing data results to design a harvester matched to the birds in testing.

2. METHODS OF HARVESTABLE POWER ESTIMATES

In order to predict the harvestable power available from a flying bird, we first must understand the total power required for flight. We use a flight power model and a known payload capacity to predict the total amount of excess power available for harvest. We then reduce this harvestable power to account for the mass of the transducer. We previously published this method of harvestable power prediction and review it here. A more detail report of the method can be found in the original paper.[1]

The power required for flight, and therefore the power available for harvest, is closely related to the mass of the bird. Models of bird flight can be used to convert flown mass to power, therefore it is important to understand how much a bird is capable of carrying in flight. There have been various attempts at quantifying the power required for flight in the past. Marden measured the maximum takeoff payload for a variety of species.[2] The results showed that most birds can take off when 16% of their flight muscles mass is added as payload. This is a large fraction of total mass of the bird and is is not sustainable, in that with this payload the birds could barely begin to fly. The United States Geological Survey (the entity responsible for managing bird banding in the U.S.) specifies that no bands or tags be placed on a bird that exceed 3% of the birds total mass[3] and Neaf-Daezner et al. showed that payloads of 3-5% could be tolerated on the coal tit (*periparus ater*) and great tit (*parus major*) without effecting survival rates.[4] Based on these results, we assume that most birds have enough excess energy such that they could continually carry up to 4% of their body mass. With this number we can now predict the amount of excess power available for harvest.

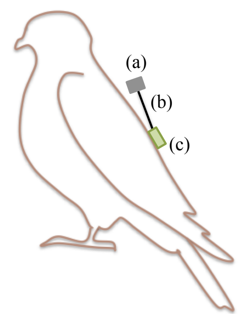

Figure 1 – Example of bird tag with attached piezoelectric vibrational power harvester. (a)Energy harvester tuning mass (b)Energy harvester (c)Mount and tag electronics

The 4% assumption for the maximum sustainable payload capacity provides a basis for the total amount of excess power. Two major bird flight power models exist.[5,6] We have chosen Pennycuick's model due to its continued refinement[7896] and relative simplicity. This model sums a variety of power expenditures required during flight. These individual power expenditures, and the equations used to predict them can be seen in table 1.

Table 1 – Power types for bird flight

Power Type	**Description**	**Equation**
Parasitic	Drag from body	$1/2\rho V^3 S_b C_{Db}$
Induced	Momentum transfer to air (lift)	$\frac{km^2g^2}{2S_dV\rho}$
Profile	Driving wings forward through flow	$\frac{C_{pro}}{A_R}\frac{1.05k^{3/4}m^{3/2}g^{3/2}S_b^{1/4}C_{Db}^{1/2}}{\rho^{1/2}B^{3/2}}$
Basal Metabolic	Caloric overhead	$\eta\alpha m^{\delta}$
Cardio/pulmonary	Cardiovascular/Breathing	1.1×sum of the others

The variables in this table can be found in the nomenclature section. From these individual power components we can calculate the total power required for flight. The power prediction depends on flight velocity. We use the velocity for minimum power expenditure (V_{mp}), as it has been shown to be the speed at which birds spend the majority of time.[10] The equations for this speed are shown in the equations below.[7]

$$V_{mp} = \frac{0.76k^{1/4}(mg)^{1/2}}{\rho^{1/2}(S_bC_{Db}S_d)^{1/4}} \tag{1}$$

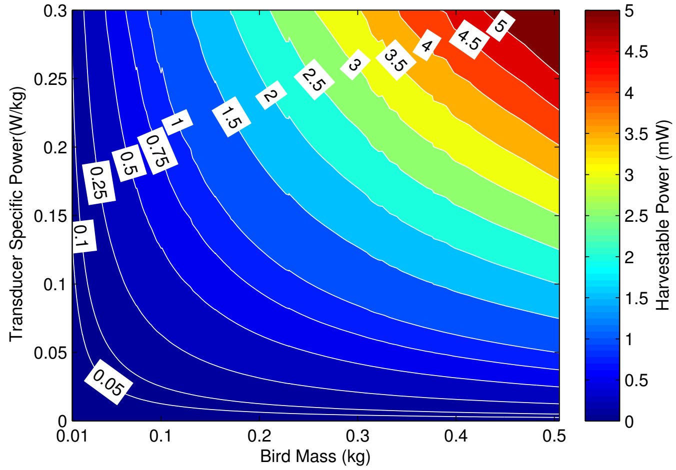

Figure 2 – Theoretical maximum harvestable power for a variety of North American birds based on the 4% maximum laden mass fraction.

Using this power model and datasets[10–12] of measured species parameters (wing span, mass, etc.), we can predict the power required for flight of a variety of bird species. We then recalculate the power required for flight, but increase the mass of each species by the 4% maximum payload. By subtracting the original power from the power required with 4% laden mass, we can calculate the available excess power. We consider this excess power the maximum power available for harvest. While this is a conservative estimate of the available power, it does not take into account the fact that the harvester itself has mass, and energy must be expended to carry it. If these affects are taken into account, the actual amount of harvestable power can be predicted by the following equation:[1]

$$P_h = \bar{P}\left(t^2 - m - m_p\right) \tag{2}$$

$$t = \frac{-B}{4A} + \frac{\pm_i W \mp_j \sqrt{-(3\lambda + 2y \pm_i \frac{2\beta}{W})}}{2} \tag{3}$$

The variables on which t depends can be found in Appendix A. We can see that there is a linear relationship between the practically harvestable power, and that of the transducer specific power. If we use the previously mentioned dataset for a variety of bird species[10–12] and calculate the practically harvestable power for a variety of transducer specific powers, we obtain the contour shown in figure 2. This figure shows that, as expected, increasing the specific power of the harvester increases the amount of power that can be safely harvested. It should also be apparent that for birds smaller than 0.1 kg, there is a strong relationship between bird mass and harvestable power. Figure 2 demonstrates the potential for vibrational energy harvesting from birds. Even for relatively low transducer specific powers, there is a significant amount of harvestable power, relative to the power requirements of modern microcontrollers.

3. FLIGHT TESTING OF ACCELERATION

In order to design an energy harvester for use on a bird, we need to size a vibrational energy harvester to a specific bird. To design these harvesters, we must know the acceleration frequency of the object to which it will be attached. In the case where the harvester is mounted to a bird, this requires the measurement of the flight accelerations. To obtain this data, we measured these flight accelerations of two species using dorsally mounted three axis accelerometers. The birds were allowed to freely fly within a flight tunnel at the University of Western Ontario's Advanced Facility for Avian Research. This tunnel is specifically designed for flight testing of birds and allows for control the airflow speed and atmospheric pressure. All tests were performed using a flight conditions that resulted in a 10 m/s sea level equivalent airspeed.

The accelerometers used in this test were part of a custom designed low-mass data logging device. The device consists of a three axis accelerometer, microcontroller (with onboard flash memory), and a battery. The accelerometer's range was ±8g with a resolution of 0.0625g. Once turned on, acceleration measurements are taken at 200Hz for 50 seconds. The logging devices weighed 443 mg and were inserted into the cradles which allowed the system to be fixed to the birds. The logging device and cradle can be seen mounted to a bird in figure 3. The total system mass with cradle and logger was 677±5mg.

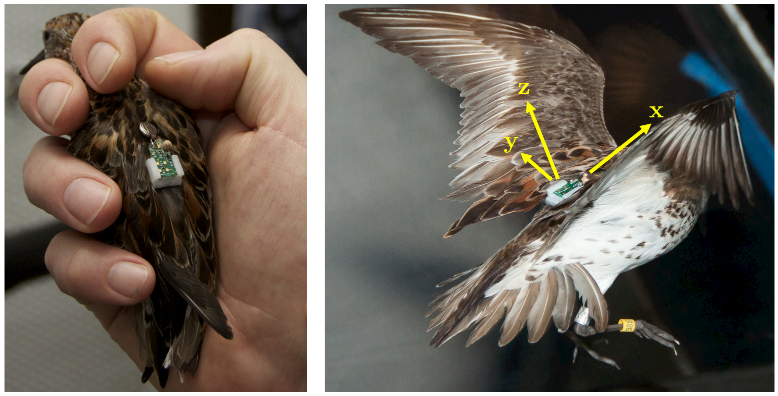

(a) (b)

Figure 3 – Data logger mounted to Western Sandpiper preflight (a) and during flight (b) with coordinate axes shown.

The testing included trials of three individual birds: one Western Sandpiper (*Calidris mauri*, WS1) and two Swainson's Thrushes (Catharus ustulatus, ST1 and ST2). WS1, ST1, and ST2 were massed at 30.11 gm, 40.75 gm, and 40.97 gm, respectively. As such the cradle and data logger assembly represented 2.25% of the mass of the Western Sandpiper, and 1.65%-1.66% of the mass of the Swainson's Thrushes. The testing procedure was as follows: The flight tunnel was brought up to 10 m/s sea level equivalent airspeed, and the birds were released near the rear of the tunnel. Flights typically consisted of birds flying toward the forward limit of the tunnel and then flying in place for the remainder of the trial. It was typical for the birds to land on the netting at the front of the tunnel prior to full the 50 seconds of data being recorded. This is the reason for the variability of the length of different trials. We concentrate here on the z-component of the acceleration measurements as this axis is perpendicular the the orientation of the energy harvester on the bird (see figure 1). Spectrograms for the three Western Sandpiper trials can be seen in Figure 4 and the four Swainson Thrush trials can be seen in Figures 5 and 6.

The z-component acceleration data presented in Figures 4-6 has been filtered through a second order high passed filtered with a cutoff frequency of 1Hz to eliminate the gravitational contribution to the data. Additionally, the spectrograms use a two second Hamming window which, due to the typical flapping frequency, represents approximately 24-28 flapping cycles. The constant window size and the variable trial times is why some of the spectrograms appear to have less resolution in time. A 1.4-1.8 second overlap was used between windows, depending on the trial. This overlap changes because it is partially based on the fundamental frequency of each trial. Adjacent to each spectrogram, is the average spectral intensity across the entire trial. Below the spectrograms is the time domain z-component acceleration data of the trial. Occasionally, the Western Sandpiper would would come into contact with the ceiling of the tunnel. These discrete events show up as brief broadband intensity in Figures 4 (a)-(c) and are part of the reason behind the average spectral intensity having more of a broadband nature than that of the Swainson's Thrush trials.

The results from the Swainson's thrush trials show spectral intensities which suggest an acceleration profile that appears more sinusoidal that that of the WS1 trials. This is especially true for the trials from ST2. In these trials, the acceleration frequency is only slightly modulated, if at all during the entirety of the trial. These two trials appear to show a slight correlation between frequency and acceleration amplitude. In Figure 6(b) we can see that as acceleration amplitude increases, there is a slight change in flapping frequency. The first

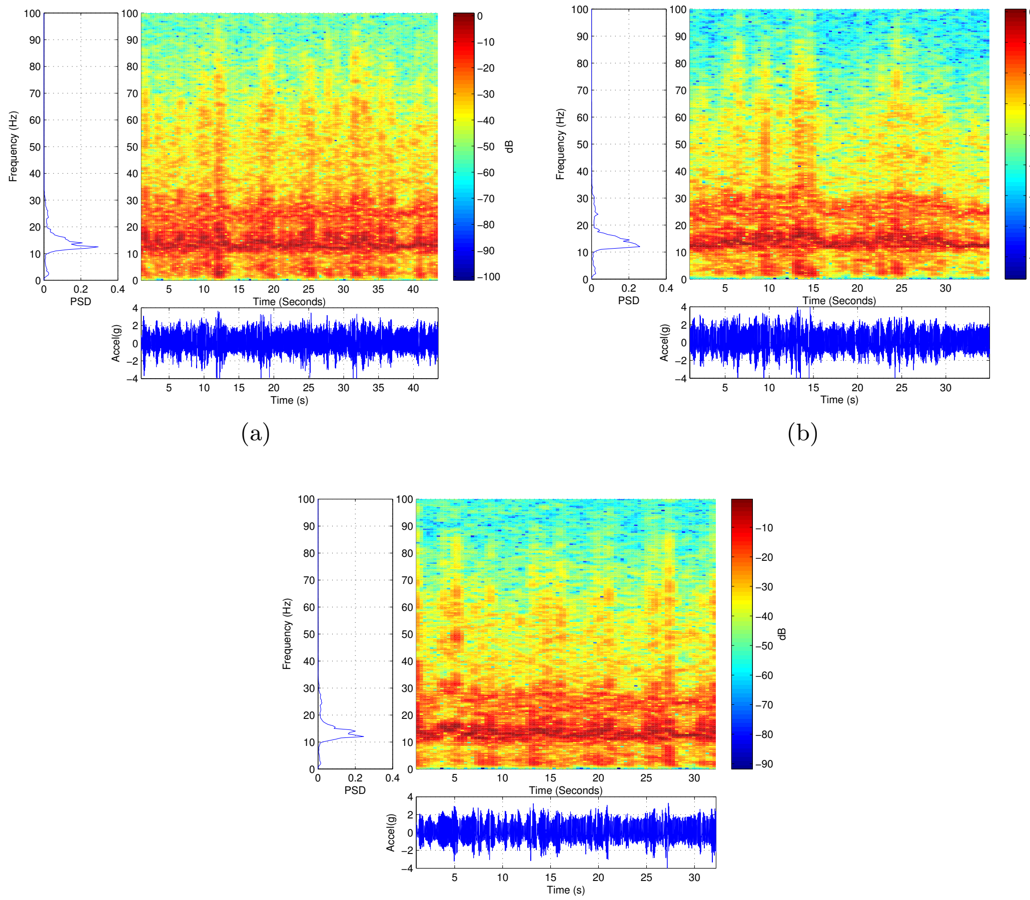

(a) (b) (c)

Figure 4 – Processed z-component acceleration data for three trials of Western Sandpiper 1. Spectrograms, average power spectral density, and high pass filtered (1Hz) raw z acceleration data

rise in amplitude in this figure (immediately after the third second) represents an increase of approximately 54%, while the flapping frequency only increases by approximately 12%. This shows that there is only a slight dependance on the flapping frequency and the flapping intensity. This is an important result, in that vibrational energy harvesters require matching the resonant frequencies. If we know that flapping frequency does not change greatly with flapping intensity, then we can expect that the flapping frequency will not change greatly with airspeed changes.

The results from Figures 4-6 show that there is a distinct flapping frequency that, although changing slightly in time does seem to center on a single frequency. Additionally, we can see that the peak acceleration amplitudes have a range of approximately $1-2$g. The average frequency and the peak accelerations are summarized in Table 2. The frequencies reported in Table 2 are based on the peak of the time average spectral intensities, shown adjacent to the spectrograms in Figures 4-6. The mean and standard deviation of the acceleration amplitude is based on a peak detection algorithm which was written specifically for this dataset.

3.1 Design of Piezoelectric Harvester

Based on the results of the acceleration test, we know that the acceleration frequency is relatively constant and that the amplitude is relatively high. We can use these facts to design piezoelectric energy harvesters for both the Western Sandpiper and Swainson's Thrushes. The design of these piezoelectric beams is based on a method developed by Shafer, Bryant, and Garcia.[13] This method was developed in order to facilitate the design of energy

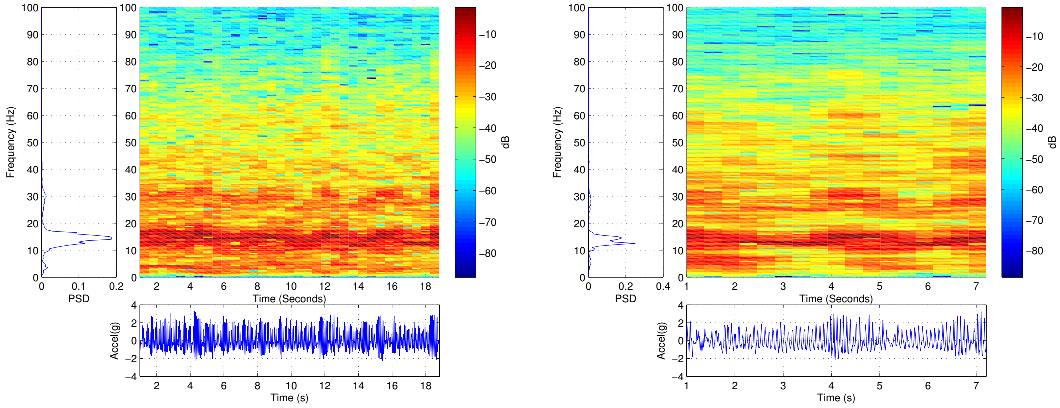

(a) (b)

Figure 5 – Processed z-component acceleration data for two trials of Swainson's Thrust 1. Spectrograms, average power spectral density, and high pass filtered (1Hz) raw z acceleration data

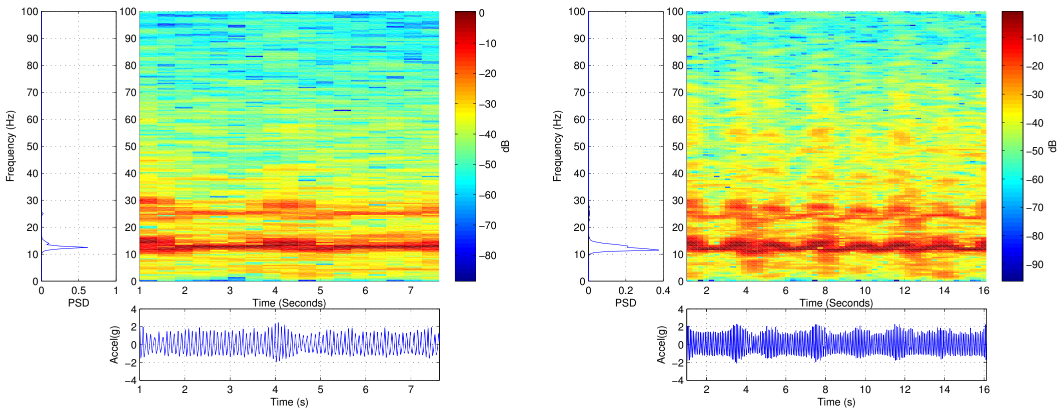

(a) (b)

Figure 6 – Processed z-component acceleration data for two trials of Swainson's Thrust 2. Spectrograms, average power spectral density, and high pass filtered (1Hz) raw z acceleration data

harvesters that have hard mass requirements. It assumes a piezoelectric bimorph with a configuration as shown in Figure 7(a). The circuit shown in Figure 7(b) is a standard model used in energy harvesting literature. The design method assumes the resistance used is matched to the ideal resistance for maximum power extraction.

The design method relies on approximations for mode shape and natural frequency. These approximations allow for the development of the expressions for the modal parameters required to predict power from the following power equation:[14]

$$P = \frac{MA^2}{\omega_n} \frac{1}{\left(r\,\Omega + \frac{\pi}{2}\right)^2} \frac{k_e^2\,\Omega^2\,r}{\left(2\zeta + \frac{2k_e^2 r}{\left(r\Omega + \frac{\pi}{2}\right)^2}\right)^2 \Omega^2 + \left(1 - \Omega^2 + \frac{\Omega\,k_e^2 r}{r\Omega + \frac{\pi}{2}}\right)^2} \tag{4}$$

Here M is the modal mass of the beam, A is the magnitude of base acceleration, ω_n is the short-circuit natural frequency of the beam, r is the non-dimensionalized load resistance, Ω is the frequency ratio, k_e^2 is the non-dimensionalized coupling coefficient, and ζ is the mechanical damping ratio. Shafer, Bryant, and Garcia develop these parameters from the approximations for natural frequency and mode shape with the following

Table 2 – Spectrogram frequency average and acceleration amplitude statistics

	Frequency (Hz)	Mean (g)	Std. Dev.(g)
WS1	12.5	1.74	0.57
	12.0	1.85	0.60
	12.0	1.67	0.54
ST1	14.5	1.65	0.63
	12.5	1.63	0.72
ST2	12.5	1.45	0.36
	11.5	1.45	0.32

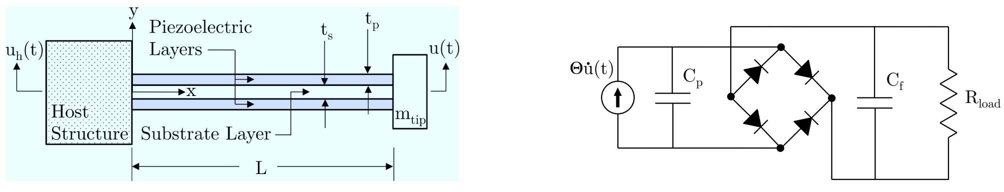

Figure 7 – (a)Typical layout of fully laminated piezoelectric energy harvester with base excitation.(b) Circuit diagram for the standard piezoelectric harvester signal rectification and dissipation.

results:

$$M = 4M_{sys} - \frac{107}{35} Ltw \left(\kappa_p \rho_p + (1-\kappa_p)\rho_s\right) \tag{5}$$

$$k_e^2 = \frac{9e^2}{8\epsilon^s E_s} \frac{\kappa_p \left(\frac{\kappa_p}{2} - 1\right)^2}{\eta \left(\kappa_p^3 - 3\kappa_p^2 + 3\kappa_p\right) + \left(-\kappa_p^3 + 3\kappa_p^2 - 3\kappa_p + 1\right)} \tag{6}$$

$$r_{sc} \approx \left(\frac{\pi^2}{\sqrt{16+\pi^2}}\right) \frac{1}{\frac{k_e^2}{\zeta}} \tag{7}$$

$$r_{oc} \approx \frac{\sqrt{16+\pi^2}}{4} \frac{\frac{k_e^2}{\zeta}}{1+k_e^2} \tag{8}$$

In these expressions L is the length of the beam, t is the total beam thickness, κ_p is the ratio of piezoelectric material thickness to beam thickness, ρ_* is material density, M_{sys} is the system mass (not modal), w is the beam width, E_* is modulus of elasticity, η is the ratio the E_p/E_s, and e and ϵ^s are the piezoelectric stress and permittivity constants. We assume here the harvester is driven at its short circuit natural frequency, such that $\Omega = 1$ and $r = r_{sc}$.

Using this method, we fix the following terms, such that the others can be solved for in terms of κ_p: system mass, natural frequency, beam length, piezoelectric thickness, and the material properties of piezoelectric and substrate materials. The system mass, in this case, is constrained by what the bird is capable of carrying. We assume here that 95% of the 4% mass limit be used to carry the energy harvester. This may initially seem illegitimate, until considering a system where the the electronics of the tag are used as the tuning mass at the tip of the energy harvester. Such design considerations are necessary when dealing with such a mass constrained system. We choose to only use 95% of this limit because we must leave some energy reserves for harvest. The natural frequency can be determined from the average of the three trials for the Western Sandpiper and the four for the Swainson's Thrushes presented in Table 2. We must also assume a beam length for the energy harvester. A length of 3 cm is legitimate, considering that the total length of the Western Sandpiper and Swainson's Thrushes range from 14-17cm and 16-19cm, respectively.[12] The substrate material is chosen to be 301 stainless steel and the piezoelectric material is Navy type II/Industry Type 5A. These constraints and the variables that are determined by the design method are presented in table 3 for both Western Sandpiper and Swainson's Thrush systems.

Table 3 – List of beam constants constraining example beam

	Western Sandpiper	**Swainson's Thrush**		
	Value	**Value**	**Unit**	**Name**
ω_1	12.2	12.8	Hz	Natural Frequency
M_{bird}	30.1	40.75	gm	Mass of Bird
M_{sys}	1.14	1.55	gm	Mass of Energy Harvester ($0.95 \times 0.04 \times M_{bird}$)
A	1.75	1.55	g	Magnitude of acceleration
L	3	3	cm	Beam Length
t_p	0.063	0.063	mm	Piezoelectric Layer Thickness
w	dependent	dependent	mm	Beam Width
ρ_s	7916.5	7916.5	kg/m^3	Substrate Density
ρ_p	7800	7800	kg/m^3	Piezoelectric Material Density
E_{s11}	212	212	GPa	Substrate Modulus
E_{p11}	67	67	GPa	Piezoelectric Material Modulus
e	-12.73	-12.73	C/m^2	Piezoelectric Stress Constant
ϵ_s	1.593e-08	1.593e-08	C/m^2	Piezoelectric Permittivity
t_s	dependent	dependent	m	Substrate Thickness
m_t	dependent	dependent	kg	Tip Mass
κ_p	variable	variable	()/()	Thickness Ratio
ζ	5	5	%	Mechanical Damping

We can see that the only variable element in table 3 is the piezoelectric thickness ratio. The terms listed as 'dependent' are determined from the fixed variables and the thickness ratio as described by Shafer, Bryant, and Garcia.[13] In this design method, the thickness ratio is swept from 0-100% and the beam that produces the maximum power is selected as the proper design. Thickness ratio was swept for the constraints in table 3 and the resulting power curves can be seen in figure 8(a). These curves have each been normalized by their individual maximums. These curve show that the both ideal designs have thickness ratios of 0.71. An example

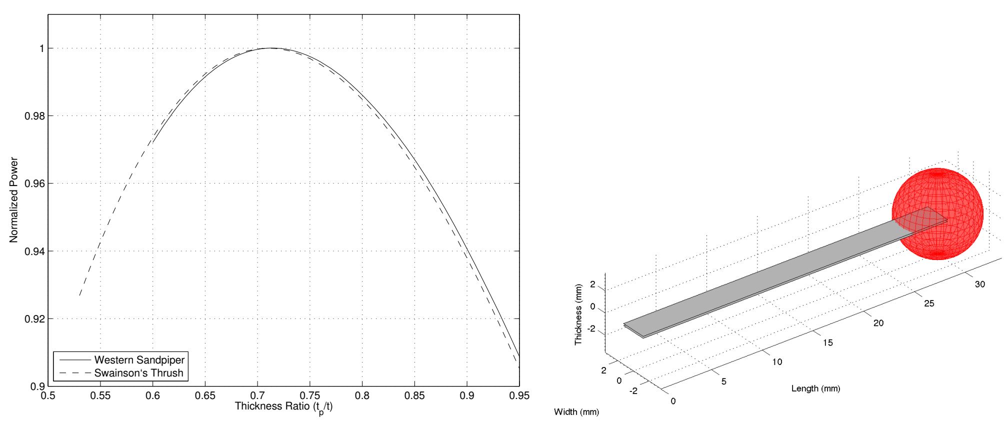

(a) (b)

Figure 8 – (a) Power vs piezoelectric thickness ratio curves for beams designed for the Western Sandpiper and Swainsons' Thrush. Note that peaks in these curves represent the ideal harvester. (b) Physical layout of ideal Swainson's Thrush piezoelectric energy harvester

of one of the ideal beam designs, that for the Swainson's Thrush, is shown in figure 8(b). The sphere at the end of the beam represents the volume of mass needed if the tip mass were made from steel. Equation 4 assumes a purely harmonic base excitation. This, in combination with the large magnitude of measured acceleration peaks in flight, conspire to produce predictions for deflection and power with are far above what would be expected for the physical system. A variety of unmodeled influences would likely reduce the deflection amplitude and power from the harvester. These include affects from the compliant nature of the beam/bird interface, the broadband nature of the acceleration signal, and viscous drag losses on the beam. For this reason it is imprudent to attempt to predict the magnitude of power using this linear model. Testing these harvesters on a flying bird would provide the best possible estimate of the specific power from these harvesters. Only then could we make predictions as to the harvester's specific power for use in comparison to figure 2.

4. CONCLUSIONS

The energy from bird flight that is available for harvest is significant and warrants consideration as a potential energy source for long life avian tracking tags. The harvestable power model based on bird power required for flight[1] is capable of providing a guideline for the maximum harvestable power if the specific power of the transducer is known. As an example case, we tested two species of birds in a flight tunnel. This was done in order to understand their flight dynamics well enough to tailor a vibrational energy harvester that would resonate at their typical flapping frequency. The results of this test showed that the birds have a flapping frequency that, although slightly varying in time, does center around a single value. Additionally, we determined that the magnitude of the acceleration of the birds in flight is on the order 1.5-1.75 g.

Using the results of the acceleration testing, we designed two harvesters for matched resonance using a design method presented by Shafer, Bryant, and Garcia.[13] These harvesters were designed such that their mass was sufficiently low as to be carried by the birds, but also matched the main flapping frequency of the birds. While the power model used does not allow for absolute predictions of the power output from these beams, future work will include fabrication of these beams for testing an flying birds.

The next step in this research is the production of a harvester for use on a flying bird. We have demonstrated that there is a significant amount of power available for harvest, and that we are capable of designing a harvester well suited for this purpose. Future work will include investigations to quantify the effect of unmodeled aspects of the bird flight in the harvester power prediction equation.

APPENDIX A. QUARTIC SOLUTION VARIABLES

$$\begin{aligned}
A &= 1.1P_{ind}^{m}/m^2 \\
B &= 1.1P_{pro}^{m}/m^{3/2} \\
C &= \bar{P} \\
E &= -1.1(1+q)^2 P_{ind}^{m} - 1.1(1+q)^{3/2} P_{pro}^{m} - \bar{P}(m+m_e) \\
\lambda &= \frac{-3B^2}{8A^2} + \frac{C}{A} \\
\beta &= \frac{B^3}{8A^3} - \frac{BC}{2A^2} + \frac{D}{A} \\
\gamma &= \frac{-3B^4}{256A^4} + \frac{CB^2}{16A^3} - \frac{BD}{4A^2} + \frac{E}{A} \\
P &= \frac{-\lambda^2}{12} - \gamma \\
Q &= \frac{-\lambda^3}{108} + \frac{\lambda\gamma}{3} - \frac{\beta^2}{8} \\
R &= \frac{-Q}{2} + \sqrt{Q^2/4 + P^3/27} \\
U &= R^{1/3} \\
y &= \begin{cases} -\frac{5}{6}\lambda + U - Q^{1/3} & \text{if } U = 0 \\ -\frac{5}{6}\lambda + U - \frac{P}{3U} & \text{if } U \neq 0 \end{cases} \\
W &= \sqrt{\lambda + 2y}
\end{aligned}$$

NOMENCLATURE

A_R	Wing aspect ratio
B	Wingspan
C_{pro}	Profile power constant-empirical
C_{Db}	Body drag coefficient
$\bar{P}$	Harvester specific power
P_h	Practical sustainably harvestable power
P_{ind}	Induced power
P_l	Laden power output
P_M	Metabolic power output
P_{par}	Parasitic drag power
P_{pro}	Profile power
S_b	Body frontal area
S_d	Circular area swept by wings
V	Forward flight velocity
g	Acceleration due to gravity
k	Induced drag factor-empirical
m	Mass of bird (unladen)
m_e	Mass of the payload (other the energy harvester)
m_p	Payload mass (other than energy harvester)
$\dot{p}$	Muscle specific power
q	Allowable fraction of laden mass (3-4%)
α	Metabolic efficiency factor
δ	Metabolic mass constant
η	Metabolic mass exponent
ρ	Air density

ACKNOWLEDGMENTS

This work was funded by both National Science Foundation grant No. CMMI-1014891 and the National Science Foundation Graduate Research Fellowship Program. The authors would additionally like to acknowledge Chris Guglielmo and Wayne Bezner at the Advanced Facility for Avian Research at the University of Western Ontario for their help with bird the flight acceleration tests.

REFERENCES

1. M. W. Shafer and E. Garcia, "Maximum and practical sustainably harvestable vibrational power from avian subjects," *ASME 2011 Conference on Smart Materials, Adaptive Structures and Intelligent Systems (SMASIS2011)* **2011**(54723), pp. 353–359, 2011.
2. J. H. Marden, "Maximum lift production during takeoff in flying animals," *Journal of Experimental Biology* **130**, pp. 235–258, 1987.
3. USGS, "How to request auxiliary marking permission." http://www.pwrc.usgs.gov/bbl/manual/aarequs.cfm, 2011. [Online; accessed February 28, 2012].
4. B. Naef-Daenzer, F. Widmer, and M. Nuber, "A test for effects of radio-tagging on survival and movements of small birds," *Avian Science* **1**(1), pp. 15–23, 2001.
5. J. M. V. Rayner, "A new approach to animal flight mechanics," *Journal of Experimental Biology* **80**(1), pp. 17–54, 1979.
6. C. Pennycuick, *Modeling the Flying Bird.*, Academic Press, 2008.
7. C. Pennycuick, "The mechanics of bird migration," *Ibis* **111**, pp. 525–556, 1969.

8. C. Pennycuick, D. S. Farner, J. R. King, and K. C. Parkes, *Avian Biology: Mechanics of Flight*, vol. 5, Academic Press, 1975.
9. C. Pennycuick, H. H. O. III, and M. R. Fuller, “Empirical estimates of body drag of large waterfowl and raptors,” *Journal of Experimental Biology* **135**, pp. 253–264, October 1988.
10. C. Pennycuick, “Actual and ’optimum’ flight speeds - field data reassessed,” *Journal of Experimental Biology* **200**, pp. 2355–2361, 1997.
11. E. L. Poole, “Weights and wing areas in north american birds,” *The Auk* **55**, pp. 511–517, July 1938.
12. Cornell_Lab_of_Ornithology, “All about birds.” http://www.allaboutbirds.org/Page.aspx?pid=1189, 2011. [Online; various search results].
13. M. W. Shafer, M. Bryant, and E. Garcia, “Designing maximum power output into piezoelectric energy harvesters,” *Smart Materials and Structures* , 2012. (In review).
14. Y. C. Shu and I. Lien, “Analysis of power output for piezoelectric energy harvesting systems,” *Smart Materials and Structures* **15**, pp. 1499–1512, September 2006a.